

Estimating the states of a dynamic system employing moving horizon estimation (MHE) based on Shor's r-algorithm optimization technique and extended Kalman filter

N. Badkoubi* and H. Jazayeri-Rad*

* Department of automation and instrumentation, Petroleum University of Technology (PUT), Tehran, Iran

Abstract—This Paper deals with estimating the states of a wastewater treatment plant (WWTP) regarding equality constraints acting on the states. First a reduced nonlinear model is presented, which is based on the rate of biomass growth in a continuous bioreactor. Then, a simulation study is performed to observe the state fluctuation of the presented model. The results of both simulation and extended Kalman filter will be depicted to demonstrate the ability of EKF as a state estimation technique. EKF is deficient in dealing with constraint problems and there is no way to involve the constraints which often act on the system. Therefore, it leads us to introduce moving horizon estimation (MHE) as a solution to this problem. MHE is actually an optimization problem which can be solved with various methods. We will introduce Shor's r-algorithm which is selected to realize this goal. Finally, the results obtained of both unconstrained extended Kalman filter and moving horizon estimation techniques are compared with each other. The result of this comparison demonstrates that in spite of possessing more processing time, MHE has less error during the period of simulation.

Keywords: Wastewater treatment; State estimation; Extended Kalman filter; Equality constraints; Moving Horizon Estimation; Shor algorithm

I. INTRODUCTION

Nitrogen removal is an important operation in wastewater treatment which commonly consists of two sub-processes: Nitrification and Denitrification. The main process is nitrification during which ammonium (NH_4^+) is oxidized to nitrate (NO_3^-) in aerobic reactor. Subsequently, Denitrification process occurs to release nitrogen gas (N_2) from (NO_3^-) in anoxic reactor [1].

The fact that internal variables which affect the system behavior are usually difficult or impossible to measure has made the scientists to establish different models to cope with this problem. The model of Hamilton [2], which includes two enzyme-related components, has been integrated into activated sludge model (ASM1) by Henze *et al* [3].

Later ASM1 model was extended to eASM by Hamilton *et al* [4] to make it feasible to deal with estimation of the parameters as well as the states of the process.

The Extended Kalman Filter (EKF) is the most widely used nonlinear state estimator which has been used for past few decades. However, EKF is deficient to deal with constraints (equality and inequality) that must be satisfied. There are different approaches to deal with the constraints which limit estimation of the states of the system [5].

In this paper we focus on MHE [5] which is an optimization-based strategy for state estimation that was first proposed by (Thomas 1975 and Kwon *et. al.* 1983). Although, it was Jang *et al.* 1986 who first proposed the unconstrained MHE as an on-line optimization strategy.

In this paper we discuss the above method to handle operating equality constraints on the wastewater pilot plant as a case study.

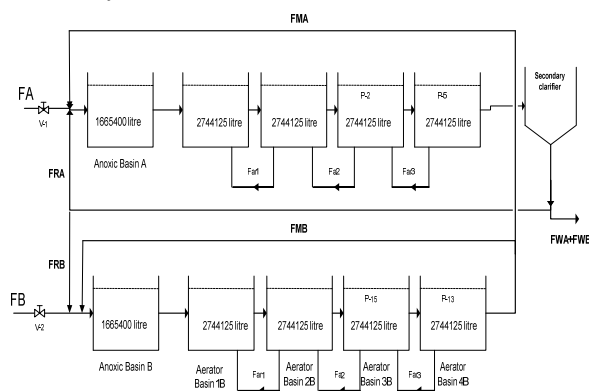


Figure 1. Hydraulic model of wastewater pilot plant.

II. PROCESS MODEL

A. Nonlinear model

The studied pilot plant was chosen from Kanapaha water reclamation facility which has been experimented by Hamilton *et. al.* [4] to estimate composition of wastewater pilot plant. The results and related data are available at:

<http://www.ees.ufl.edu/homepp/koopman/hamilton.etal2>

The simplified hydraulic model of the plant is shown in Figure 1. It is assumed that there is one anoxic basin and four aerobic basins in series in two trains and one secondary

Corresponding author: Department of automation and instrumentation, Petroleum University of Technology (PUT), Iran, Tehran, South Hasan Banna St. , Masil Bakhtar St., No.36 , Tel.:+98 913 3019008; Fax:+98 611 5551754 E-mail address: n.badkoubi@gmail.com (Nima Badkoubi)

clarifier which the sludge flow out of the system after qualifying sludge retention time (SRT). Information about intra-facility dilution streams was used to calculate the biomass concentrations entering the process by diluting the standard wastewater composition are given in Table I [4].

TABLE I. INFLUENT WASTEWATER COMPOSITION

Component	Symbol	Units	Value
Soluble inert substrate	S_I	gCOD/m ³	62
Particulate inert substrate	X_I	gCOD/m ³	62
Readily degradable substrate	S_S	gCOD/m ³	99
Slowly degradable particulate substrate	X_S	gCOD/m ³	247
Nitrate plus nitrite nitrogen	S_{NO}	gN/m ³	0
Ammonia nitrogen	S_{NH}	gN/m ³	24
Soluble degradable organic nitrogen	S_{ND}	gN/m ³	4
Particulate degradable organic nitrogen	X_{ND}	gN/m ³	6
Active heterotrophic biomass	$X_{B,H}$	gCOD/m ³	0
Active autotrophic biomass	$X_{B,A}$	gCOD/m ³	0
Inert decay products	X_P	gCOD/m ³	0
Alkalinity	S_{ALK}	gmol/m ³	6
Dissolved oxygen	S_O	gCOD/m ³	0
Nitrate reductase	E_N	kat ^a /L	0
Intracellular nitrate	$S_{NO,i}$	g/L	0

Values taken from potter et al.(1996).

^aKatlas (moles substrate reduced per second).

The changing rate of each composition of the wastewater is calculated by:

$$\frac{dX}{dt} = \text{advection} + \text{reaction_rate} + \text{mass transfer} \quad (1)$$

where the advection (bulk flow) terms are described by a hydraulic model, the reaction terms by a biochemical model and the mass transfer term describes the action of the aerators. Equation (2) gives the anoxic basin advection expression for particulate material. The term X_{setunf} is the component concentration of underflow layer of the settler which is recycled back to the anoxic basin to save energy and cost. It is assumed that the concentrations of soluble components in the fourth aerobic basin and all layers of the settler (see Figure 4) including the underflow to the anoxic basin are equal [15].

$$\frac{dX_{an}}{dt} = \frac{F_A X_{influent}}{V_{an}} + \frac{F_{RA} X_{setunf}}{V_{an}} + \frac{F_{MA} X_{b4}}{V_{an}} - \frac{(F_{MA} + F_A + F_{RA}) X_{an}}{V_{an}} \quad (2)$$

The advection terms for virtual aerobic reactors are defined in Equations (3) to (6):

$$\frac{dX_{b1}}{dt} = \frac{(F_{MA} + F_A + F_{RA}) X_{an}}{V_{b1}} + \frac{F_{ar1} X_{b2}}{V_{b1}} - \frac{(F_{MA} + F_A + F_{RA} + F_{ar1}) X_{b1}}{V_{b1}} \quad (3)$$

$$\frac{dX_{b2}}{dt} = \frac{(F_{MA} + F_A + F_{RA} + F_{ar1}) X_{b1}}{V_{b2}} + \frac{F_{ar2} X_{b3}}{V_{b2}} - \frac{F_{ar1} X_{b2}}{V_{b2}} - \frac{(F_{MA} + F_A + F_{RA} + F_{ar2}) X_{b2}}{V_{b2}} \quad (4)$$

$$\frac{dX_{b3}}{dt} = \frac{(F_{MA} + F_A + F_{RA} + F_{ar2}) X_{b2}}{V_{b3}} + \frac{F_{ar3} X_{b4}}{V_{b3}} - \frac{F_{ar2} X_{b3}}{V_{b3}} - \frac{(F_{MA} + F_A + F_{RA} + F_{ar3}) X_{b3}}{V_{b3}} \quad (5)$$

$$\frac{dX_{b4}}{dt} = \frac{(F_{MA} + F_A + F_{RA} + F_{ar3}) X_{b3}}{V_{b4}} - \frac{F_{ar3} X_{b4}}{V_{b4}} - \frac{(F_{MA} + F_A + F_{RA}) X_{b4}}{V_{b4}} \quad (6)$$

The reaction rate is the sum of twelve different processes each of which include several ingredients depicted in Table II. Therefore, the reaction rate for the ingredient i will be:

$$\text{Rate}_i = \sum_j V_{ij} \rho_j \quad (7)$$

where ρ_j is the j^{th} process rate and V_{ij} is the i^{th} component of the j^{th} process of the ingredients matrix $V_{15 \times 12}$ in Table II.

The mass transfer component of the overall balance equation describes the rate at which the surface aerators are able to introduce dissolved oxygen into the aerobic basin. The mass transfer for oxygen is given below, where the index i represents the number of aerobic basin. The value for K_{LA2} is derived from performance per horsepower specifications from the manufacturer and the performance for the remaining aerators was found by fitting ASM1 to the KWRF nutrient data.

$$\frac{dS_{O_i}}{dt} = K_{LA_i} (S_{O,sat} - S_{O_i}) \quad (8)$$

Activated sludge plants transform organic matter into biomass. The effective operation of the process requires the biomass to be removed from the liquid stream (in the secondary settler) prior to being discharged in the receiving waters. The sedimentation of the particles in the liquor is achieved by gravity along with the density differences between the particles and the liquid. Part of the biomass is purged, while a large fraction is returned to the biological reactor to maintain the appropriate substrate-to-biomass ratio. This means that the settler combines functions of clarification and thickening into one unit, as shown in Figure 2. In some cases the settler model can perform more important tasks, such as sludge storage or reactions.

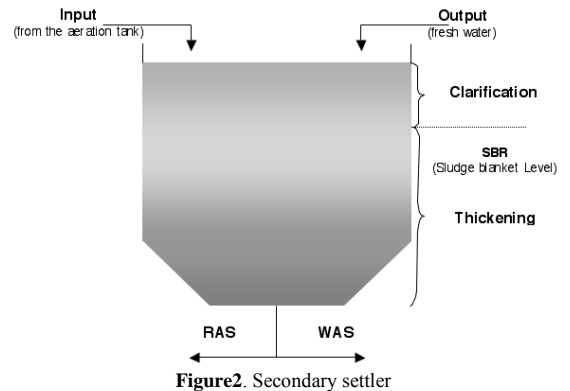


Figure2. Secondary settler

The model considers only one state variable for all of the particulate components (the solids concentration) and all the soluble state variables, leaving the settler without settling.

The model was extended to include the clarification zone (not included by Strenstrom) by Vitasovic in 1985 [14]. The settler was divided into ' n ' layers (see Figure 4) with the feed entering in layer ' m '. It is assumed the feed is instantaneously

and completely distributed throughout the feed layer. Thus, the region below the feed level is modeled according to Strenstrom's approach and the clarification zone represented according to the Vitasovic's extension of the model.

In Figure 3, the simplified flow scheme is shown. At the inlet section the inflow and the solids concentration are homogeneously spread over the horizontal cross section, and the incoming solids are distributed uniformly and instantaneously across the entire cross-sectional area. The flow is divided into a downward flow towards the underflow outlet at the bottom, and an upward flow.

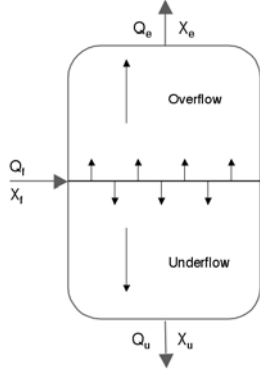


Figure 3. Influent distribute homogeneously through feed layer

B. Reduced model

We simplified the model to be able to define some constraints embedding all 5 basins of train A. In this paper we are interested in the concentration of active heterotrophic biomass $X_{B,H}$ and active autotrophic biomass $X_{B,A}$. Hereby, we reduce the number of 5×15 differential equations of 5 basin of train A to 10 by choosing $X_{B,H}$, $X_{B,A}$ as the main ingredients of the processes among all 15 ingredients. Therefore, the related reactions for each basin occur as below:

$$r_{XB,H} = \hat{\mu}_H \left(\frac{S_s}{k_s + S_s} \right) \left(\frac{S_O}{k_{O,H} + S_O} \right) X_{B,H} + \hat{\mu}_H \frac{E_N}{E_{N,max}} \frac{S_{NO,j}}{S_{NO,j,max}} \left(\frac{S_s}{k_s + S_s} \right) \eta_g X_{B,H} - b_H X_{B,H} \quad (9)$$

$$r_{XB,A} = \hat{\mu}_A \left(\frac{S_{NH}}{k_{NH} + S_{NH}} \right) \left(\frac{S_O}{k_{O,A} + S_O} \right) X_{B,A} - b_A X_{B,A} \quad (10)$$

The mass balance in each reactor can be written as:

$$\frac{dX_i}{dt} = \text{advection}_i + \text{reaction_rate}_i \quad (11)$$

All states of reduced order model are summarized in Table III. These equations will be used later in Kalman state estimation. $X_{inluent}$ is a scaled concentration entering the process by diluting the standard wastewater composition and V_x is the volume of x^{th} basin in Figure 1.

TABLE II. EASM1M MODEL

Component i →	Process j ↓	1	2	3	4	5	6	7	8	9	10	11	12	13	14	15	Process Rate, ρ_j ; $ML^{-3}T^{-1}$
1	Aerobic growth of heterotrophs		$-\frac{1}{V_H}$			1											$\hat{\mu}_H \left(\frac{S_s}{k_s + S_s} \right) \left(\frac{S_O}{k_{O,H} + S_O} \right) X_{B,H}$
2	Anoxic growth of heterotrophs		$-\frac{1}{V_H}$			1											$\hat{\mu}_H \frac{E_N}{E_{N,max}} \frac{S_{NO,j}}{S_{NO,j,max}} \left(\frac{S_s}{k_s + S_s} \right) \eta_g X_{B,H}$
3	Aerobic growth of autotrophs						1			$\frac{1}{V_A}$	$-\dot{X}_{B,H} - \frac{1}{V_A}$						$\hat{\mu}_A \left(\frac{S_{NH}}{k_{NH} + S_{NH}} \right) \left(\frac{S_O}{k_{O,A} + S_O} \right) X_{B,A}$
4	Decay of heterotrophs							f_P					$\dot{X}_{B,H} - f_P \dot{X}_{B,H}$				$b_H X_{B,H}$
5	Decay of autotrophs							f_P					$\dot{X}_{B,A} - f_P \dot{X}_{B,A}$				$b_A X_{B,A}$
6	Ammonification of soluble organic nitrogen										1	-1		$\frac{1}{V_A}$			$k_a S_{ND} X_{B,A}$
7	Hydrolysis of entrapped organics																$k_h \frac{X_s}{k_X + (X_s/V_{B,H})} \left[\left(\frac{S_O}{k_{O,H} + S_O} \right) + \gamma_h \left(\frac{K_{OH}}{k_{O,H} + S_O} \right) \left(\frac{S_{NO}}{k_{NO} + S_{NO}} \right) \right] X_{B,H}$
8	Hydrolysis of entrapped organic nitrogen											1	-1				$P_T (X_{ND}/X_S)$
9	Uptake of nitrate																$V_{EN} \frac{E_N}{E_{N,max}} \left(\frac{S_{NO}}{k_{NO} + S_{NO}} \right) \left(\frac{K_{OH}}{k_{O,H} + S_O} \right) \left(\frac{S_s}{k_s + S_s} \right) X_{B,H}$
10	Synthesis of nitrate reductase														1		$\alpha \eta \left(\frac{X_{B,H} f_{EN} S_{NO,j}}{k_{EN} + X_{B,H} + V_{EN} S_{NO,j}} \right) \left(\frac{S_s}{k_s + S_s} \right) X_{B,H}$
11	Decay of intracellular nitrate																$b_S S_{NO,j}$
12	Decay of nitrate reductase																$b_{EN} E_N$

Observed conversion rates, $ML^{-3}T^{-1}$ $r_i = \sum_j \nu_{ij} \rho_j$

TABLE III. STATES OF REDUCED ORDER MODEL	
1)	$\frac{dX_{B,Hon}}{dt} = \frac{F_A}{V_{an}} X_{B,H inf luent} + \frac{F_{RA}}{V_{an}} X_{B,H underflow} + \frac{F_{M4}}{V_{an}} X_{B,Hb-4} - \frac{(F_{M4} + F_A + F_{RA})}{V_{an}} X_{B,Hon} + J_{XB,H(on)}$
2)	$\frac{dX_{B,Aon}}{dt} = \frac{F_A}{V_{an}} X_{B,A inf luent} + \frac{F_{RA}}{V_{an}} X_{B,A underflow} + \frac{F_{M4}}{V_{an}} X_{B,Ab-4} - \frac{(F_{M4} + F_A + F_{RA})}{V_{an}} X_{B,Aon} + J_{XB,A(on)}$
3)	$\frac{dX_{B,Hob1}}{dt} = \frac{(F_A + F_{RA} + F_{M4})}{V_{ob1}} X_{B,Hon} + \frac{F_{ob1}}{V_{ob1}} X_{B,Hob2} - \frac{(F_{M4} + F_A + F_{RA} + F_{ob1})}{V_{ob1}} X_{B,Hob1} + J_{XB,H(ob1)}$
4)	$\frac{dX_{B,Aob1}}{dt} = \frac{(F_A + F_{RA} + F_{M4})}{V_{ob1}} X_{B,Aon} + \frac{F_{ob1}}{V_{ob1}} X_{B,Aob2} - \frac{(F_{M4} + F_A + F_{RA} + F_{ob1})}{V_{ob1}} X_{B,Aob1} + J_{XB,A(ob1)}$
5)	$\frac{dX_{B,Hob2}}{dt} = \frac{(F_A + F_{RA} + F_{M4} + F_{ob1})}{V_{ob2}} X_{B,Hob1} + \frac{F_{ob2}}{V_{ob2}} X_{B,Hob3} - \frac{F_{ob2}}{V_{ob2}} X_{B,Hob2} - \frac{(F_{M4} + F_A + F_{RA} + F_{ob2})}{V_{ob2}} X_{B,Hob2} + J_{XB,H(ob2)}$
6)	$\frac{dX_{B,Aob2}}{dt} = \frac{(F_A + F_{RA} + F_{M4} + F_{ob1})}{V_{ob2}} X_{B,Aob1} + \frac{F_{ob2}}{V_{ob2}} X_{B,Aob3} - \frac{F_{ob2}}{V_{ob2}} X_{B,Aob2} - \frac{(F_{M4} + F_A + F_{RA} + F_{ob2})}{V_{ob2}} X_{B,Aob2} + J_{XB,A(ob2)}$
7)	$\frac{dX_{B,Hob3}}{dt} = \frac{(F_A + F_{RA} + F_{M4} + F_{ob2})}{V_{ob3}} X_{B,Hob2} + \frac{F_{ob3}}{V_{ob3}} X_{B,Hob4} - \frac{F_{ob3}}{V_{ob3}} X_{B,Hob3} - \frac{(F_{M4} + F_A + F_{RA} + F_{ob3})}{V_{ob3}} X_{B,Hob3} + J_{XB,H(ob3)}$
8)	$\frac{dX_{B,Aob3}}{dt} = \frac{(F_A + F_{RA} + F_{M4} + F_{ob2})}{V_{ob3}} X_{B,Aob2} + \frac{F_{ob3}}{V_{ob3}} X_{B,Aob4} - \frac{F_{ob3}}{V_{ob3}} X_{B,Aob3} - \frac{(F_{M4} + F_A + F_{RA} + F_{ob3})}{V_{ob3}} X_{B,Aob3} + J_{XB,A(ob3)}$
9)	$\frac{dX_{B,Hob4}}{dt} = \frac{(F_A + F_{RA} + F_{M4} + F_{ob3})}{V_{ob4}} X_{B,Hob3} - \frac{F_{ob4}}{V_{ob4}} X_{B,Hob4} - \frac{(F_{M4} + F_A + F_{RA})}{V_{ob4}} X_{B,Hob4} + J_{XB,H(ob4)}$
10)	$\frac{dX_{B,Aob4}}{dt} = \frac{(F_A + F_{RA} + F_{M4} + F_{ob3})}{V_{ob4}} X_{B,Aob3} + \frac{F_{ob4}}{V_{ob4}} X_{B,Aob4} - \frac{(F_{M4} + F_A + F_{RA})}{V_{ob4}} X_{B,Aob4} + J_{XB,A(ob4)}$

The expression for reaction rates and value of parameters that were used in this work are all given in [4].

The model is based on the solid flux concept, which states that the solids entering the secondary settler are carried to the bottom via the gravity settling flux (J_s) and the bulk flux (J_b). The first is resulted from the sludge settling downward through the water, whereas the second is from the water moving downward in the settler owing to the underflow sludge recycle pump. The total flux is given by:

$$J = J_s + J_b \quad (12)$$

Five different groups of layers are represented in the Vitasovic's model depending on their position relative to the feed point: the top layer and the layers above the feed point (clarification zones); the feed layer; the layers below feed point; and the bottom layer (thickening zones). These layers can be modeled as:

- Top layer:

$$\frac{dX_{10}}{dt} = \frac{V_{up}(X_9 - X_{10}) - J_{clar,10}}{Z_{10}} \quad (13)$$

- Clarification zone (Above feed layer)

$$\frac{dX_m}{dt} = \frac{V_{up}(X_{m-1} - X_m) + J_{clar,m+1} - J_{clar,m}}{Z_m} \quad (14)$$

- Feed layer

$$\frac{dX_m}{dt} = \frac{\frac{Q_f X_f}{A} - (V_{up} + V_{dn})X_m + J_{clar,m+1} - \min(J_{s,m}, J_{s,m-1})}{Z_m} \quad (15)$$

- Thickening zone

$$\frac{dX_m}{dt} = \frac{V_{dn}(X_{m+1} - X_m) + \min(J_{s,m}, J_{s,m+1}) - \min(J_{s,m}, J_{s,m-1})}{Z_m} \quad (16)$$

- Bottom layer

$$\frac{dX_1}{dt} = \frac{V_{dn}(X_2 - X_1) + \min(J_{s,1}, J_{s,2})}{Z_1} \quad (17)$$

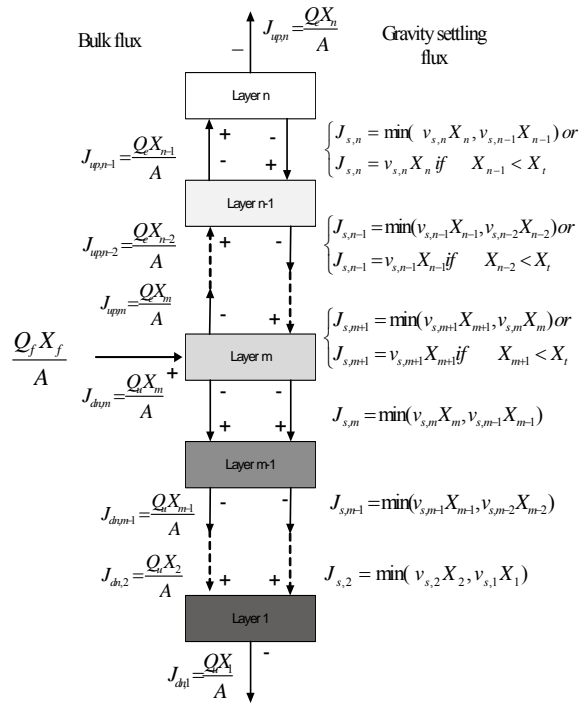


Figure 4. Traditional one dimensional layer settler model

where Z_i is the depth of the i^{th} layer of the settler. We assumed that all layers have the same depth of 0.46 meter. Additionally, $J_{clar,m}$ is the gravity settling flux for the m^{th} layer calculated as:

$$J_{clar,m} = \begin{cases} \min(v_{s,n} X_n, v_{s,n-1} X_{n-1}) & \text{if } X_{n-1} > X_t \\ v_{s,n} X_n & \text{if } X_{n-1} < X_t \end{cases} \quad (18)$$

where the threshold concentration X_t is equal to 3000 g.m⁻³ and is adopted from the BSM1 benchmark [15].

To calculate the distribution of particulate concentrations in the recycle and the wastage flows, their ratios with respect to the total solid concentration are assumed to remain constant across the settler [16]:

$$\frac{X_{ing,f}}{TSS_f} = \frac{X_{ing,unf}}{TSS_{unf}} \quad (19)$$

where TSS_f and $X_{ing,f}$ are the influent concentrations of TSS and the specified particle to the settler respectively. Also, TSS_{unf} and $X_{ing,unf}$ correspond to the similar parameters in the underflow of the settler. Note that this assumption means that the dynamics of the fractions of particulate concentrations in the inlet of the settler will be directly propagated to the settler underflow and overflow, without taking into account the normal retention time in the settler [15].

Moreover, initial values of total suspended solid values of 10 layers were adopted from Hamilton experiment based on the Kanapaha wastewater treatment plant [4]. Figure 5 depicts the variation of total suspended solid in the period of simulation for underflow, feed and top layers respectively. It is shown that the amount of TSS increases until it reaches to a

steady value. Please note that there is a sinusoidal harmonic in the picture which is made of sinusoidal origin of the influent flow to the system.

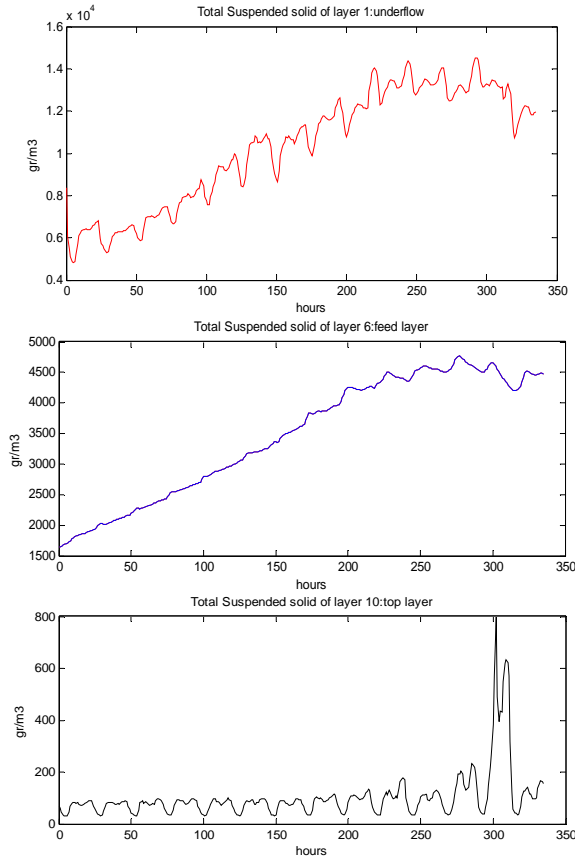


Figure 5. Total suspended solid concentration for bottom layer for 2 weeks of simulation

C. Nonlinear constraints on the system

Although EKF is the most popular means of estimating the states for nonlinear systems, it is not able to cope with constraints problem such as $g(x) = h$.

Constraints are additional conditions which act on the states and show the limits of states variation because of physical property of the system or desired operating programs.

In the steady-state case the sludge retention time (SRT) calculation is based on the total amount of biomass present in the system, i.e. the reactor and the settler [15], [17]:

$$SRT = \frac{TX_a + TX_s}{\phi_e + \phi_w} \quad (20)$$

where TX_a is the total amount of biomass present in the reactor:

$$TX_a = \sum_{i=1}^{i=n} (X_{B,H,i} + X_{B,A,i}) V_i \quad \text{with } n=5 \quad (21)$$

TX_s is the total amount of biomass present in the settler:

$$TX_s = \sum_{i=1}^{i=m} (X_{B,H,i} + X_{B,A,i}) z_i \cdot A \quad \text{with } m=10 \quad (22)$$

ϕ_e is the loss rate of biomass present in the settler:

$$\phi_e = (X_{B,H,m} + X_{B,A,m}) Q_e \quad (23)$$

where $m=10$ and ϕ_w is the loss rate of biomass in the wastage flow:

$$\phi_w = (X_{B,H,u} + X_{B,A,u}) Q_w \quad (24)$$

On the basis of laboratory tests and actual operating data, it has been found that a SRT of about 3 to 15 days results in the production of a stable, high quality effluent sludge with excellent settling characteristics [17] and [18]. In this work we take a value of SRT equal to 10 days and this is then used to estimate the states under the specified SRT constraint.

III. UNCONSTRAINT STATE ESTIMATION

As explained earlier the wastewater pilot plant is governed by continuous-time dynamics whereas the measurements are obtained at discrete instants of time. Hybrid EKF [6] is a special format of EKF that deals with these types of systems.

The complete reduced nonlinear model describing ammonia mass balance can be written in the following state space equations:

$$\begin{aligned} \dot{x} &= f(x, u, t) + w(t) \\ y_k &= h_k(x_k) + v_k \\ w(t) &= (0, Q) \\ v_k &= (0, R_k) \end{aligned} \quad (25)$$

where x is presented by equations (1) to (10) of Table III, and

$$y_k = x_4(k) + v_k \quad (26)$$

Additionally, $w(t)$ is a continuous white noise with covariance Q that was taken to be equal to $0.6I_{5 \times 5}$, and the measurement noise v_k is a discrete white noise with covariance R_k assumed to be 0.6 for the accuracy of ammonia probe in the third Aerobic basin.

The rate of states and related error covariance can be written as:

$$\begin{aligned} \dot{\hat{x}} &= f(\hat{x}, u, t) \\ \dot{P} &= F(t)P(t) + P(t)F(t) + Q \end{aligned} \quad (27)$$

where F is the Jacobian of f with respect to the state vector. We need to discretize the differential algebraic equation (25) conceptually in order to perform any computation or analysis as below:

$$\begin{aligned} x_{k+1} &= Fx_k + w_k \\ y_k &= H_k x_k + v_k \\ w_k &= (0, Q_k) \\ v_k &= (0, R_k) \end{aligned} \quad (28)$$

where k denotes the discrete-time index. A typical choice is $t = k\Delta T_s$ where ΔT_s is sampling period that in our simulation, it assumed to be equal to one hour. Additionally, H_k is the Jacobian of $h(x_k)$ with respect to the state vector. A

posteriori state vector (\hat{x}_k^+) and error covariance (P_k^+) are calculated as below:

$$\begin{aligned} K_k &= P_k^- H_k^T (H_k (\hat{x}_k^-) P_k^- H_k^T (\hat{x}_k^-) + R)^{-1} \\ \hat{x}_k^+ &= \hat{x}_k^- + K_k [y_k - h(\hat{x}_k^-)] \\ P_k^+ &= [I - K_k H_k (\hat{x}_k^-)] P_k^- \\ \hat{x}_{k+1}^- &= \hat{x}_k^+ + \mathcal{G}_k \\ P_{k+1}^- &= P_k^+ + \mathcal{P}_k \end{aligned} \quad (29)$$

K_k is the Kalman gain of EKF. The Initial states and covariance matrices were assumed as:

$$P_0^- = \begin{bmatrix} \begin{matrix} X_{B,H-an} \\ X_{B,A-an} \\ X_{B,H-ab1} \\ X_{B,A-ab1} \\ X_{B,H-ab2} \\ X_{B,A-ab2} \\ X_{B,H-ab3} \\ X_{B,A-ab3} \\ X_{B,H-ab4} \\ X_{B,A-ab4} \end{matrix} & \begin{matrix} x_{1,0}^- \\ x_{2,0}^- \\ x_{3,0}^- \\ x_{4,0}^- \\ x_{5,0}^- \\ x_{6,0}^- \\ x_{7,0}^- \\ x_{8,0}^- \\ x_{9,0}^- \\ x_{10,0}^- \end{matrix} & \begin{matrix} 396.0834 \\ 46.0340 \\ 424.8892 \\ 47.3046 \\ 427.0126 \\ 47.5217 \\ 426.2335 \\ 47.4283 \\ 425.5722 \\ 47.3828 \end{matrix} \\ \begin{matrix} 400 & 0 & 0 & 0 & 0 & 0 & 0 & 0 & 0 & 0 & 0 \\ 0 & 10 & 0 & 0 & 0 & 0 & 0 & 0 & 0 & 0 & 0 \\ 0 & 0 & 400 & 0 & 0 & 0 & 0 & 0 & 0 & 0 & 0 \\ 0 & 0 & 0 & 10 & 0 & 0 & 0 & 0 & 0 & 0 & 0 \\ 0 & 0 & 0 & 0 & 400 & 0 & 0 & 0 & 0 & 0 & 0 \\ 0 & 0 & 0 & 0 & 0 & 10 & 0 & 0 & 0 & 0 & 0 \\ 0 & 0 & 0 & 0 & 0 & 0 & 400 & 0 & 0 & 0 & 0 \\ 0 & 0 & 0 & 0 & 0 & 0 & 0 & 10 & 0 & 0 & 0 \\ 0 & 0 & 0 & 0 & 0 & 0 & 0 & 0 & 400 & 0 & 0 \\ 0 & 0 & 0 & 0 & 0 & 0 & 0 & 0 & 0 & 0 & 10 \end{matrix} \end{bmatrix}$$

A comparison between simulated states and EKF estimator is depicted in Figures 6 and 7. In these figures both simulation and extended Kalman filtered results have been shown for each of the reactors in the anoxic and four aerobic basins. To simulate this model numerically, Matlab software was used [12].

IV. CONSTRAINT STATE ESTIMATION

Suppose $g(x_k) = h$ is a nonlinear constraint on state vector, as proved by Dan Simon [5], the nonlinear constraint can be expanded by Taylor series around \hat{x}_k^- to obtain a linearized constraint

$$\begin{aligned} Dx_k &= d \\ D &= \mathcal{G}(\hat{x}_k^-) \\ d &= h - g(\hat{x}_k^-) + \mathcal{G}(\hat{x}_k^-) \hat{x}_k^- \end{aligned} \quad (30)$$

where the D matrix is a known $s \times n$ matrix ($s < n$).

A. Moving Horizon Estimation technique

From the perspective of probability theory, state estimation means the conditional probability density function of the states

$\{x_0, x_1, \dots, x_T\}$ given the measurements $\{y_0, y_1, \dots, y_{T-1}\}$ where $T-1$ is time of the current measurement [9],[10].

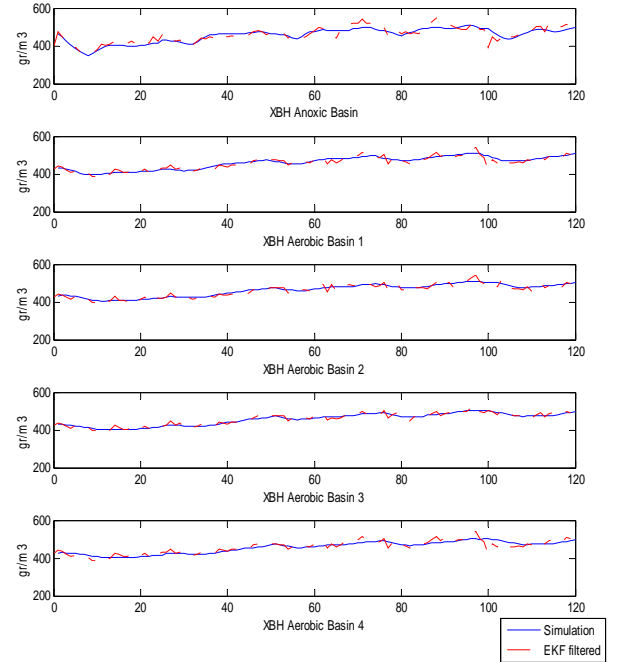


Figure6. A comparison between EKF and simulation for concentration of heterotrophs $X_{B,H}$ for all basins

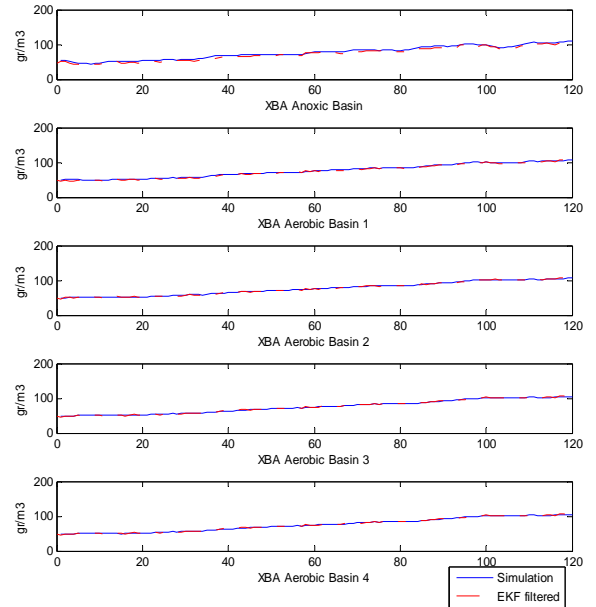


Figure7. A comparison between EKF and simulation for concentration of autotrophic $X_{B,A}$ for all basins

$$p(x_0, x_1, \dots, x_T | y_0, y_1, \dots, y_{T-1}) \quad (31)$$

The optimal estimate of the state at time k is denoted as $\hat{x}_{k|T-1}$ and is a function of conditional probability density function (30). A typical choice for this function is maximum *a posteriori* estimate:

$$\left\{ \hat{x}_{0|T-1}, \hat{x}_{1|T-1}, \dots, \hat{x}_{T|T-1} \right\} = \underset{\{x_0, x_1, \dots, x_T\}}{\operatorname{argmin}} p(x_0, x_1, \dots, x_T | y_0, y_1, \dots, y_{T-1}) \quad (32)$$

This can be interpreted to the following optimization problem [5], [9], [10]:

$$\left\{ \hat{x}_k^+ \right\} = \underset{\{x_k\}}{\operatorname{argmin}} \|x_0 - \hat{x}_0\|_{P_0^{-1}}^2 + \sum_{k=0}^{T-1} \|x_{k+1} - Fx_k\|_{Q^{-1}}^2 + \sum_{k=0}^{T-1} \|y_k - Hx_k\|_{R^{-1}}^2 \quad (33)$$

where $\left\{ \hat{x}_k^+ \right\} = \left\{ \hat{x}_{0|T-1}, \hat{x}_{1|T-1}, \dots, \hat{x}_{T|T-1} \right\}$, and F & H are Jacobians of process model and measurement model respectively, regarding state vector of the process. This optimization problem can be solved by quadratic programming that is explained in [12]. To handle increasing dimension of mathematical optimization problem (32), it is required to limit the bound of optimization as next measurements are received [10]. So, the modified moving horizon estimator is written as:

$$\left\{ \hat{x}_k^+ \right\} = \underset{\{x_k\}}{\operatorname{argmin}} \|x_M - \hat{x}_M^+\|_{(P_0^+)^{-1}}^2 + \sum_{k=T-M}^{T-1} \|x_{k+1} - Fx_k\|_{Q^{-1}}^2 + \sum_{k=T-M}^{T-1} \|y_k - Hx_k\|_{R^{-1}}^2 \quad (34)$$

where M presents the horizon length. In other words, MHE accounts only for the last M measurements and the window of estimating moves forward as a new measurement arrives.

To deal with the constraints discussed earlier in section IV and to obtain the optimal states vector, the optimization problem can be altered as:

$$\left\{ \hat{x}_k^+ \right\} = \underset{\{x_k\}}{\operatorname{argmin}} \|x_M - \hat{x}_M^+\|_{(P_M^+)^{-1}}^2 + \sum_{k=T-M}^{T-1} \|x_{k+1} - Fx_k\|_{Q^{-1}}^2 + \sum_{k=T-M}^{T-1} \|y_k - Hx_k\|_{R^{-1}}^2 \quad \text{such that } z(\{x_k\}) = 0 \quad (35)$$

where $z(x_k) = g(x_k) - h$.

To solve this optimization problem the "SolvOpt" Matlab program written by Alexei *Kuntsevich* and Franz *Kappel* [13] was used. "SolvOpt" apply Shor's *r*-algorithm which is elaborated in the next section.

The size of the horizon is a compromising solution between estimation accuracy and computational effort. Results for the state estimation using MHE in comparison with extended Kalman filter are shown in Figures 8 and 9.

B. Shor's *r*-algorithm technique

Shor's *r*-algorithm seems to be one of the most efficient methods for the minimization of non-smooth (i.e., almost-differentiable) functions [19].

The main idea of the algorithm is to make steps in the direction opposite to a sub-gradient at the current point. However, the steps are to be made in the transformed space.

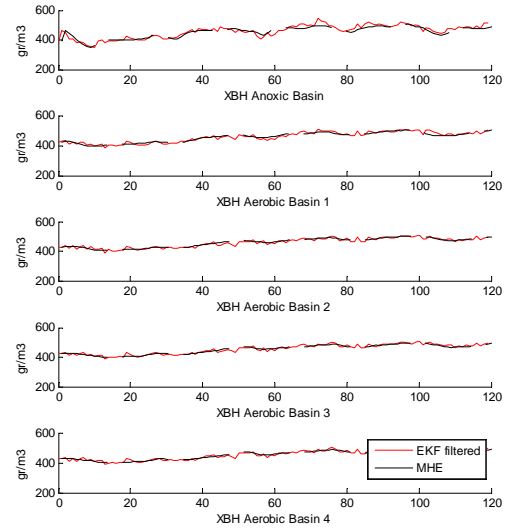


Figure8. A comparison between EKF and moving horizon estimation for concentration of heterotrophs $X_{B,H}$ for all basins

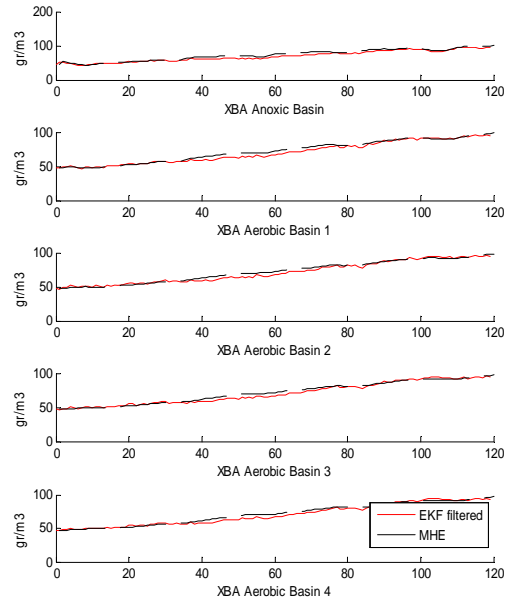


Figure9. A comparison between EKF and moving horizon estimation for concentration of autotrophic $X_{B,A}$ for all basins

The way to perform this transformation is quite simple. In each iteration, one calculates the difference between a sub-gradient at the current point and that calculated at the previous step. The direction obtained is used to perform dilation of the space with a given a priori as coefficient $\alpha > 1$.

Let $f(\cdot)$ be an almost-differentiable convex function defined on \mathbb{R}^n which is differentiable on its domain except on a set of measure zero. Let us denote an almost-gradient of $f(\cdot)$ at the point x by $g_f(x)$. Consider the following iterative algorithm (steps 1 through 9 below) for minimization of the function $f(\cdot)$.

Assume that after k iterations one has obtained the point x_k , the space transformation matrix B_k and the sub-gradient \tilde{g}_k of the function $\varphi_k(y) = f(B_k y)$ at the point $\tilde{y} = B_k^{-1} x_{k-1}$.

At the $(k+1)$ -th iteration the following calculations have to be performed:

- 1- Calculate $g_f(x_k)$, a sub-gradient f at x_k .
- 2- Calculate $g_k^* = B_k^T g_f(x_k)$ a sub-gradient of φ_k at $y_k = B_k^{-1} x_k$.
- 3- Calculate $r_k = g_k^* - \tilde{g}_k$, the difference of the two sub-gradients of φ_k at y_k and \tilde{y}_k .
- 4- Set $\xi_{k+1} = r_k / \|r_k\|$. The normalized vector ξ_{k+1} is the direction of the next space dilation to be performed.
- 5- Calculate $B_{k+1} = B_k R_\beta(\xi_{k+1})$, where $\beta = 1/\alpha$. The matrix $R_\beta(\xi_{k+1})$ is the inverse of $R_\alpha(\xi_{k+1})$, the matrix of the space dilation in the direction ξ_{k+1} with coefficient α given by:
$$R_\alpha(\xi_{k+1})x = x + (\alpha - 1)(x^T \xi_{k+1})\xi_{k+1}, \quad x \in \mathbb{R}^n \quad (36)$$
- 6- Calculate $\tilde{g}_{k+1} = B_{k+1}^T g_f(x_k)$ that is a sub-gradient of the function $\varphi_{k+1}(y) = f(B_{k+1} y)$ at the point $\tilde{y}_{k+1} = B_{k+1}^{-1} x_k$.
- 7- Choose a step size h_{k+1} .
- 8- Set $x_{k+1} = x_k - h_{k+1} B_{k+1} \tilde{g}_{k+1}$.
- 9- Check the stopping criterion and stop if it is satisfied, otherwise proceed to the next iteration.

To turn the r -algorithm as presented above into an efficient and robust optimization routine, one has to find solutions to the following problems:

- Initialization and re-initialization of the space transform matrix B_k and initialization of the step size h_k .
- Choice of the step size h_{k+1} to optimize the efficiency of space dilation in the direction of two consecutive sub-gradients (of the transformed function φ_k).
- Construction of a stopping criterion which does not need information on gradients.

For detail information please see manual script for ‘‘SolvOpt’’ program [13].

V. RESULTS

Accumulated RMS constraint error (see equation 37) recorded for 7 days of simulation and the time of processing for estimation of ammonia nitrogen is shown in Table IV. The

total data of ammonia probe measurements for the whole period of simulation (7 days with 1 hour as sampling period) was utilized in each filtering technique in a real time manner. The accumulated RMS error for all sampled data, RMS_{error} , and the initial constraint value, $E_N(x)$, were calculated as:

$$RMS_{error} = \sqrt{\sum_{N=1}^T (E(x_N) - E(x_0))^2} \quad (37)$$

$$E(x_N) = \frac{\sum_{i=1}^{i=N} (X_{B,H,i} + X_{B,A,i})V_i + TX_s}{\phi_e + \phi_w} - 10 \quad (38)$$

where T is the total duration of simulation.

In Table IV, it is shown that MHE results in a lower amount of accumulated RMS error and a higher amount of processing time than the corresponding outcomes of EKF in the period of the experiment. It should be noted that the elapsed computation time was measured in a PC with a CPU clock of 3GHz.

TABLE IV. DIFFERENT METHOD OF CONSTRAINED STATE ESTIMATION		
Method	Accumulated Constraint RMS Error	Elapsed time
Unconstrained EKF	1.0e+003 * 1.3212	115.1 s
Moving Horizon estimation	1.0e+003 * 0.2050	127.5 s

VI. CONCLUSION

Although extended Kalman filter is a powerful technique to estimate the states of the system for processes where a direct measurement of the states is not possible, it is deficient to deal with constraint problems. We discussed the MHE method to cope with this constraint problem acting on a reduced nonlinear wastewater model. It was then verified that MHE has a superior capability to deal with this issue than a conventional method.

ACKNOWLEDGMENT

I would like to thank Dr. Ryan Hamilton for providing access to real data of Kanapaha waste water treatment plant.

REFERENCES

- [1] J. Dosta, A. Gali', T. Benabdallah El-Hadj, S. Mace', and J. Mata-A'lvarez, "Operation and model description of a sequencing batch reactor treating reject water for biological nitrogen removal via nitrite", *Bioresource Technology*, vol. 98, pp. 2065–2075, 2007.
- [2] R. Hamilton, A. Casasu's, M. Rasche, A. Narang, S. A. Svoronos, and B. Koopman, "Structured Model for Denitrifier Diauxic Growth", *Wiley InterScience*, 2005.
- [3] M. Henze, W. Gujer, T. Mino, and M.V., Loosdrecht, "Activated sludge models ASM1, ASM2, ASM2d and ASM3. Scientific and Technical Report no. 9. International Water Association", London, England, 2000.

- [4] R. Hamiltona, B. Braunb, B. Koopmanc, and S. A. Svoronosa, "Estimation of nitrate reductase enzyme parameters in activated sludge using an extended Kalman filter algorithm", *Water Research*, vol. 42, pp. 1889 – 1896, 2008.
- [5] D. Simon, "Kalman Filtering with State Constraints How an optimal filter can get even better", January 18, 2008, available at <http://academic.csuohio.edu/simond/ConstrKF>
- [6] D. Simon, "Optimal State Estimation". New York: John Wiley & Sons, 2006.
- [7] D. Simon and T. Chia, "Kalman filtering with state equality constraints," *IEEE Transactions on Aerospace and Electronic Systems*, vol. 38, no. 1, pp. 128-136, 2002.
- [8] B. Teixeira, J. Chandrasekar, L. Torres, L. Aguirre, and D. Bernstein, "State estimation for linear and nonlinear equality-constrained systems," submitted for publication", *Decision and Control*, 2007 46th IEEE Conference, pp. 6220 – 6225, 12-14 Dec. 2007.
- [9] C. V. Rao, J. B. Rawlings, and J. H. Lee, "Constrained linear state estimation-a moving horizon approach", *Automatica*, vol. 37, pp. 1619-1628, 2001.
- [10] Christopher V. Rao, and James B. Rawlings Constrained Process Monitoring: Moving-Horizon Approach, *AICHE Journal*, Vol. 48, No. 1, January 2002.
- [11] T. Kraus, P. Kuhl, L. Wirsching, H. G. Bock, and M. Diehl, "A Moving Horizon State Estimation algorithm applied to the Tennessee Eastman Benchmark Process", *IEEE International Conference on Multisensor Fusion and Integration for Intelligent Systems Heidelberg*, Germany, September 3-6, 2006.
- [12] Optimization Toolbox, MATLAB software, the mathworks Inc. available www.mathworks.com
- [13] Optimization program Solvopt available at: <http://www.kfunigraz.ac.at/imawww/kuntsevich/solvopt/content.html>
- [14] Z. Z. Vitasovic. "An integrated control strategy for the activated sludge process", PhD thesis, Rice University, Houston, Texas, 1986.
- [15] IWA Task Group on Benchmarking of Control Strategies for WWTPs <http://www.benchmarkWWTP.org>
- [16] I. Takacs, G. G. Patry, and D. Nolasco, "A dynamic model of the clarification-tickening process", *Water Research*, vol. 25, no.10, pp.1263–1271, 1991.
- [17] M. Mulas, "Modelling and Control of Activated Sludge Processes", PHD thesis, Universit' a degli Studi di Cagliari, 2006.
- [18] Meltcalf & Eddy Inc. "Wastewater Engineering: treatment, disposal and reuse", McGraw Hill, 1991.
- [19] N.Z. Shor, "Minimization Methods for Non-Differentiable Functions, Springer Series in Computational Mathematics", Springer-Verlag, Berlin, vol. 3, 1985.